Influence of solar dryer inlet configuration on the energy process efficiency

Hakim SEMAI[#1], Amor BOUHDJAR[*2], Sofiane El MOKRETAR[*3]

Centre de Développement des Energies Renouvelables, CDER.

B.P.62, Route de l'Observatoire, Bouzaréah, Alger, 16340, Algérie.

[1]h.semai@cder.dz

[2]a.bouhdjar@cder.dz

[3]s.elmokretar@cder.dz

Abstract— **The present work is a comparative study between two solar dryer models. The first model is a conventional dryer that serves as a reference model and the second dryer is the one on which some geometric shape changes have been made. The main modification is to raise the dryer above the ground for about a 20 cm height and to consider the lower surface of the pebble bed as the access of air inside the drying chamber, unlike the reference model in which the air access is made on the front side with an opening of 20 cm in height and 2 m in width. The pebble bed porosity is about 40%. The simulation is performed using a CFD code which focuses on a typical day with its weather conditions i.e. solar radiation and ambient temperature changing all along. The dryer in question will operate empty, without any product to dry. The study will thus define the best efficiency obtained for both models of solar dryers operating in direct mode and by natural convection.**

Keywords—**Solardryer, solar collector,heat storage, turbulent flow, unsteady flow**

I. INTRODUCTION

Today, solar radiation is an important alternative source of energy. It is relatively preferred to other sources because it is abundant, inexhaustible, clean and free compared to the rising prices and shortages of fossil fuels [1]. Solar drying is one of the applications that benefit more from free solar energy. Farmers dry crops, in particular dates, mint and tomatoes, by lying them into thin layers, on mats, paved floor or on the ground, thereby exposing them to the sun. This process is not very hygienic. It depends on weather conditions and there is a risk of deterioration [2].

Some of the problems associated with the drying in the open air can be resolved by the use of a solar dryer which reduces crop losses and improves significantly the dried product quality compared to traditional methods of drying [3]. Several studies have been conducted in the field of drying and, particularly, solar drying. Experimental and theoretical studies have contributed the improvement of the techniques used in solar drying and precisely the performance of such dryers.

Design and solar dryer components depend on the amount, the type and the classification of the product to be dried.

Research has focused on the conditions that help improve the drying process such as increasing the amount of solar energy recovered through the greenhouse effect or improving the flow and thus the energy transport through the drying air particularly by enhancing the chimney effect for example in the drying by natural convection.

H.Semai et al. [8] studied the effect of the wind flow on the energy efficiency of a solar dryer while adopting different geometric shapes on this dryer. Decreasing the ratio of the width to the thickness of the collector and by setting up a front edge system of the surface of the glass would reduce losses to the outside of the collector.

H. Semai et al. [9] performed a comparative study between two solar dryers. The first dryer is a reference dryer. On the second one, some changes have made on its geometric shape. A first modification is to shift the updraft chimney towards the centre of the glazing. The second change is to bring the entry of the chimney to the surface of the rack, and give it a form comparable to that of a hood. The simulation is carried out using a CFD code.

The dryer in question operates empty of any product to dry. The walls of the chimney are considered semi-transparent in order to avoid the effect of shade on the collector surface. Such changes improved the energy efficiency of the dryer.

Forson & al. [10] presented a mathematical model on the drying of the agricultural products in a solar drier operating in mixed mode using a single pass and double air-water duct into the air collector. The model was developed in parallel with the experimental work. The model includes the heating air process, the drying process and evaluation techniques of the performance criteria. The results of the experimental data used for validation of the model are presented. Thus, the results of the simulation result tests obtained with the model are presented and compared to experimental data.

To get more insight about solar dryer configuration, the chosen configurations of the solar dryers will be studied through the evolution of the air flow in the drying chamber, and its passing through the drying rack. So we will determine

the configuration that would allow us obtain a heat transfer fluid with a higher absorption capacity (lower humidity).

II. SIMULATION DOMAIN

The simulation domain is limited to the dryer envelop, the ground surface, an inlet and an exit of the field which are taken far from the location of the dryer. An inlet air velocity is imposed at the entrance of the field as well as a temperature equivalent to the ambient temperature. On leaving the area, a condition type "OUT FLOW" is prescribed. The semitransparent walls feature an absorbance coefficient of 0.64 value. The sidewalls and the bottom wall of the dryer are assumed adiabatic. Figure 1 shows the solar collector with an inlet air situated at a 0.2 m height from the ground and figure 2 shows the solar dryer where fluid access to the drying chamber takes place through the bottom surface of the pebble bed. At the entrance of the domain, inlet conditions defined by the speed of the wind flow and the ambient temperature prescribed. Specific climate conditions i.e. Tizi Ouzou region are considered.
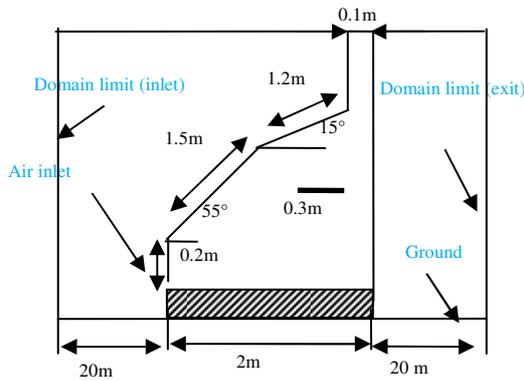
Fig. 1 solar dryer with the entrance at a 0.2 m height.
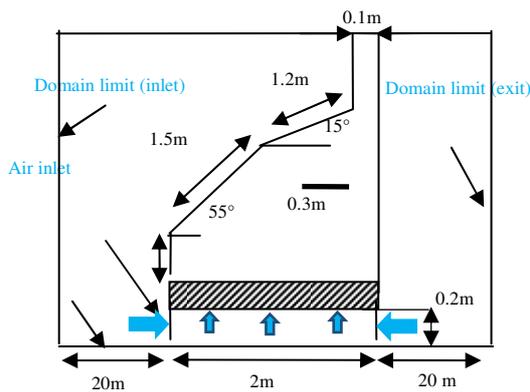
Fig. 2 solar dryer with the entrance at the bottom surface under the pebble bed.

In the experimental study of the wind flow characteristics [11], the adopted velocity profile is a logarithmic profile. In the Prandtl formulation, the mixed average length l_m is introduced.

The momentum vertical flux is given, at any moment, by:

$$\rho \cdot \overline{u'w'} = -\rho \cdot l_m^2 \cdot \left(\frac{\partial u}{\partial z}\right)^2 (1)$$

Prandtl assumed that the flux density of the momentum is constant throughout the flow. This is equivalent to the shear stress $\tau \,(\text{kg.m}^{-1}\text{s}^{-2})$ and τ_0 is the shear stress near the ground surface orwall stress which is the driving force exerted by the wind on the surface, equal and opposite to the braking force exerted by the surface, then we have:

$$\tau_0 = \tau = -\rho \cdot \overline{u'w'} \qquad (2)$$

Putting: $u^* = \sqrt{\tau_0/\rho}$ also called friction speed
and $l_m = k.z$
                    (3)
By combining equations (1), (2) and (3), we get the partial differential equation for the wind vertical profile.

$$\frac{\partial u}{\partial z} = \frac{u^*}{k.z} \quad (4)$$

Integration of this equation gives us the logarithmic profile of the wind speed in a turbulent boundary layer:

$$u(z) = \frac{u^*}{k} \cdot ln\left(\frac{z}{z_0}\right) \qquad (5)$$

$u^* = \sqrt{\tau/\rho}$: friction speed, z0 : roughness parameter, κ=0.41: Van Karman constant.
for a temperature of 15°C, ρ_{air}=1.23 kg.m^{-3}, Haxaire found a wall shear stress :
$\tau_0 = \rho. \overline{u'. w'} = 0.0411 \text{ kg.m}^{-1}.\text{s}^{-2}$ and $u^* = 0.183 \; m/s$

A linear regression and an identification of z_0 by the least square method generated the soil roughness parameter:
z_0= 0.2158m. [12].
Thus we will use the logarithmic speed profile defined by the following equation:

$$u(z) = \frac{u^*}{k} \cdot ln\left(\frac{z}{z_0}\right) = 0.45 * ln\left(\frac{z}{0.2158}\right) \qquad (6)$$

III. MATHEMATICAL MODEL

The generated mathematical model is defined under the following assumptions:

- The side walls being reflective and isolated, heat exchanges are assumed unidirectional vertically.
- The storage system put in place which is the pebble bed has a porosity of 40% of the total volume.

- The soil temperatures, walls and indoor air are assumed uniform.
- Conduction in the glass wall is insignificant through its thickness.
- The diffuse solar flux is considered isotropic.
- The air which is the working fluid is assumed viscous, Newtonian and follows Bousinesq approximation [12].
- The fluid properties are assumed constant.

The governing equations for the fluid flow are given by:

- Continuity equation

$$\frac{\partial \rho}{\partial t} + \frac{\partial (u_i)}{\partial x_i} \qquad (7)$$

- Momentum equations

$$\frac{\partial u_i}{\partial t} + u_j \frac{\partial u_i}{\partial u_j} = -\frac{1}{\rho}\frac{\partial p}{\partial x_i} + \vartheta \left(\frac{\partial^2 u_i}{\partial x_j x_j}\right) + \rho f \qquad (8)$$

with f, the body force

- Energy equation

$$\frac{\partial}{\partial t}(\rho c_p T) + \frac{\partial}{\partial x_j}(\rho u_j c_p T) = \frac{\partial}{\partial x_j}\left(\lambda \frac{\partial T}{\partial x_j}\right) + T\beta\frac{\partial p}{\partial t} + \emptyset \qquad (9)$$

with

$\emptyset$: internal energy source term

$$\emptyset = 2\mu\delta_{ij}\frac{\partial u_i}{\partial x_j} - \frac{2}{3}\mu(\nabla.u)^2\delta_{ij} \qquad (10)$$

- Transport equations for K-ε standard model [13]

$$\frac{\partial}{\partial t}(\rho K) + \frac{\partial}{\partial x_i}(\rho K u_i) = \frac{\partial}{\partial x_j}\left(\left(\mu + \frac{\mu_t}{\sigma_k}\right)\frac{\partial K}{\partial x_j}\right) + G_k + G_b - \rho\varepsilon - Y_M + S_k \qquad (11)$$

$$\frac{\partial}{\partial t}(\rho\varepsilon) + \frac{\partial}{\partial x_i}(\rho\varepsilon u_i) = \frac{\partial}{\partial x_j}\left(\left(\left(\mu + \frac{\mu_t}{\sigma_\varepsilon}\right)\frac{\partial \varepsilon}{\partial x_j}\right)\right) + C_{1\varepsilon}\frac{\varepsilon}{K}(G_k + C_{3\varepsilon}G_b) - C_{2\varepsilon}\rho\frac{\varepsilon^2}{K} + S_\varepsilon \qquad (12)$$

G_K is the turbulent kinetic energy generated by the average velocity gradient, which is evaluated in the case of the Boussinesq approximation by:

$$G_k = \mu_t S^2 \qquad (13)$$

$$S = \sqrt{2S_{ij}S_{ij}} : \text{deformation rate and } S_{ij} = \frac{1}{2}\left(\frac{\partial u_i}{\partial u_j} + \frac{\partial u_j}{\partial u_i}\right) \qquad (14)$$

G_b is the turbulent kinetic energy generated by the gravitational effect.

$$G_b = \beta g_i \frac{\mu_t}{P_{rt}}\frac{\partial T}{\partial x_i} \qquad (15)$$

with

the turbulent viscosity $\quad \mu_t = \rho C_u \frac{K^2}{\varepsilon} \qquad (16)$

and the turbulent Prandtl number $\quad P_{rt} = 0.85$

Y_M is the parameter related to the volumetric expansion of a compressible fluid.

$C_{1\varepsilon} = 1.44, \ C_{2\varepsilon} = 1.92, C_u = 0.09, \ \sigma_k = 1, \sigma_\varepsilon = 1.3, \ C_{3\varepsilon} = \tan|{}^V\!/_u|$ [14].

IV. RESULTS AND INTERPRETATION

The following figures represent the results obtained using meteorological data (solar radiation and ambient temperature) that evolve along the day.

On Figure 3, the turbulent kinetic energy at a height of 5 cm from the drying rack is represented with respect to time. The maximum value of the turbulent kinetic energy is obtained at the drier with the air inlet at the base of the pebble bed and the minimum value is obtained at the reference dryer. The turbulent kinetic energy is an indication about the turbulence intensity and this, therefore, increases the mixing capacity of the system and promotes more the heat exchange. Thus, the result shows that a better fluid mixing is obtained in the dryer whose configuration has the air inlet to the drying chamber at the base of the pebble bed.

On Figure 4, the average velocity profiles of the upward air flow in both dryer models at the chimney entrance are given. The resulting velocities are almost uniform all along the day but with values which differ from one case to another. The velocities are less important in the case of the dryer with the air inlet in the drying chamber at the basis of the dryer. Maximum speeds are recorded in the reference dryer. Speed values, in both dryer models, get higher with an increase in solar radiation. Thus, we notice that the reference dryer model generates higher speed values of the air compared the ones given by the flow in the modified one at the base of the chimney.
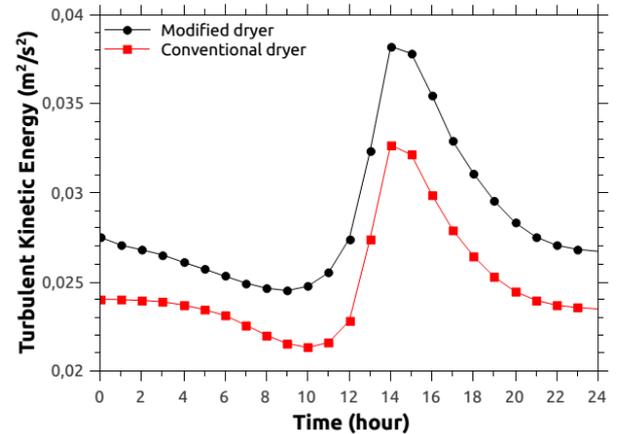
Fig. 3 Average turbulent kinetic energy intensity at 5 cm from drying rack
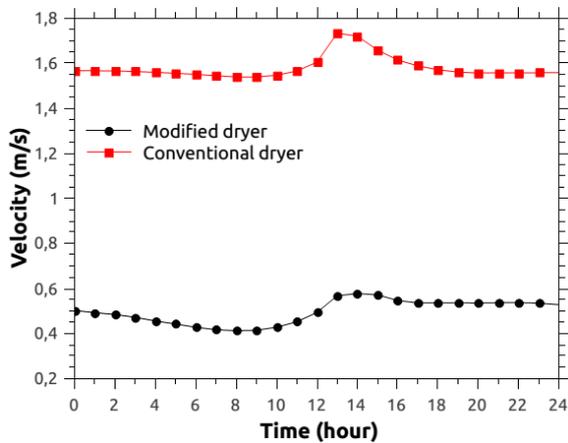
Fig. 4 Flow average speed at the inlet chimney section

Figure 5 and Figure 6 give the average temperatures at 5 cm above the drying rack and inside the drying room, respectively. Both temperature profiles evolve similarly. The maximum temperature values are obtained when solar radiation reaches its peak (after the zenith time) and are particularly important in the case of the collector with the base as the input. In the first hours after sunrise, temperatures recorded in the two dryers are similar.

Also, as it can be seen, the process keeps on for several hours in the absence of the only source of energy (solar radiation) and this is due to storage system in place, made by the pebble bed.
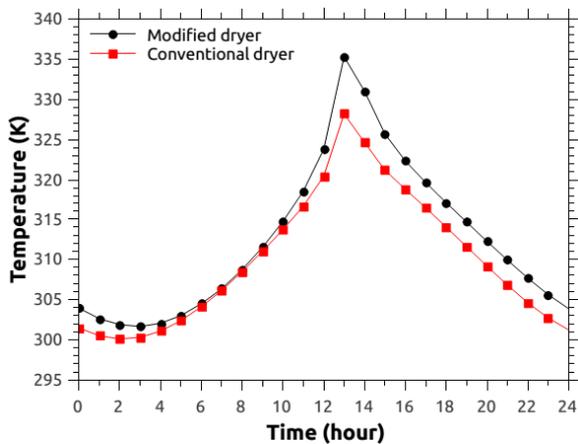
Fig.5 Average temperatures in the drying rack

Figure 7 shows ambient temperature and solar radiation for a typical day of May. Thus, we can see that the maximum temperature reaches 303 K and the maximum value of solar radiation is close to 900 W/m2.
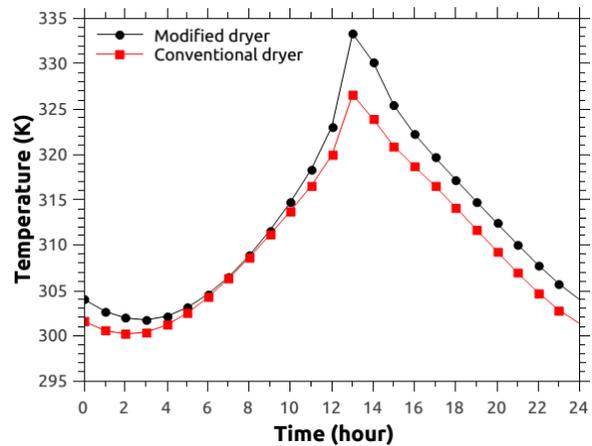
Fig. 6 Average temperatures in the drying room

The results found, especially the inside drying chamber temperatures, are closer to those found in the works of S. El Mokretar et al. [15] in their experimental studies on the energy and mass balance in a greenhouse type dryer.
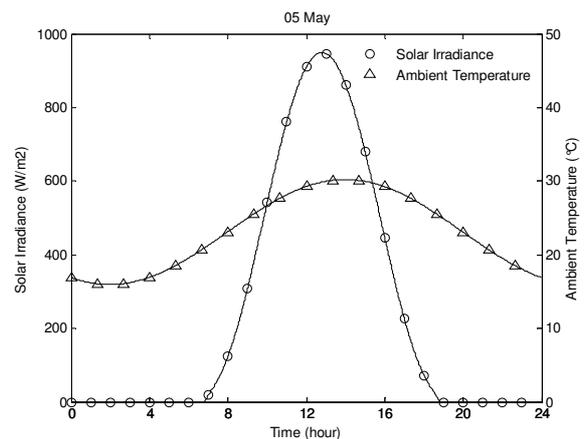
Fig.7 Solar irradiance (W/m2) and ambient temperature (K) for a typical day of May

V. CONCLUSION

The modeling study of the two models of dryers allowed us to monitor the fluid flow within the two collector models and to determine which of the two collectors generates better performance.

However, fluid access to the drying room through the base of the pebble bed has generated, according to the analysis:

➢ A higher turbulence at the drying rack, which enhances further the heat exchange between the product to be dried and the flowing fluid.

➢ An increase in the fluid temperature inside the drying room and in the drying rack and, particularly, during the most sunny period of the day. However, few hours after sunrise, temperatures are almost identical in both dryer types.

➢ A decrease in flow speed leading to a decrease in the fluid flow rate. Depending on the product characteristics, this will affect seriously the drying time and therefore the efficiency of said dryer.

NOMENCLATURE

Cp : specific heat at constant pressure[$KJ.Kg^{-1} .K^{-1}$]
G: gravitational acceleration[$m.s^{-2}$]
K: kinetic energy of turbulence [$J.Kg^{-1}.m.s^{-2}$]
L: characteristic length [m]
P: pressure [Pa]
Pr: Prandtl number
Ra: Rayleigh number
S: source term
T: temperature, [K]
t: time[s]
u, v, w: Velocity Components [$m.s^{-1}$]
u*: friction velocity [$m.s^{-1}$]
u': speed fluctuation [$m.s^{-1}$]
x, y, z: independent variables [m]
z_0: roughness parameter [m]

Greek symbols
λ: thermal conductivity [$W.m^{-1}.K^{-1}$]
α: thermal diffusivity[$m^2.s^{-1}$)]
ε: turbulent dissipation rate [$m^2 s^{-3}$]
μ: dynamic viscosity [$kg.m^{-1}.s^{-1}$]
β: volume expansion coefficient [K^{-1}]
∅: internal energy dissipation source [w]
ρ: density [$kg.m^{-3}$]
$δ_{ij}$: Chronecker symbol

Subscript, superscript
t: turbulent

REFERENCES

[1] Basunia, M.A., Abe, T. Thin layer solar drying characteristics of rough rice under natural convection. Journal of Food Engineering 47 (4): 295–301, 2001.

[2] Bala, B.K., Mondol, M.R.A., Biswas, B.K., Das Chowdury, B.L., Janjai, S. Solar drying of pineapple using solar tunnel drier. Renewable Energy 28: 183–190, 2003.
Madhlopa, A., Ngwalo, G. Solar dryer with thermal storage and biomass back-up heater. Solar Energy 81: 449–462, 2007.

[3] Ekechukwu, O.V., Norton, B., 1997. Experimental studies of integral-type natural-circulation solar-energy tropical crop dryers. Energy Conversion and Management 38 (14), 1483–1500.

[4] Sodha, M.S., Bansal, N.K., Kumar, Ashvini, Bansal, P.K., Malik, M.A.S., 1986. Solar Crop Drying. CRC Press, New York.

[5] Murthy, M.V.R., 2009. A review of new technologies, models and experimental investigations of solar driers. Renewable and Sustainable. Energy Reviews 13 (4), 835–844.

[6] Pangavhane, D.R., Sawhney, R.L., 2002. Review of research and development work on solar dryers for grape drying. Energy Conversion and Management 43, 45–61.

[7] H. SEMAI & al. Effet de l'écoulement du vent sur le rendement d'un séchoir solaire suivant une géométrie adoptée, Congrès national de mécanique des fluides (CNMF). USTHB - ALGER, 2012.

[8] H. SEMAI & al. Effet de la cheminée sur le rendement d'un séchoir solaire. 16èmes JournéesInternationales de Thermique (JITH 2013) Marrakech (Maroc), 2013.

[9] F.K. Forson, M.A.A. Nazha, H. Rajakaruna. Modelling and experimental studies on a mixed-mode natural convection solar crop-dryer. Solar Energy 81; 346–357, 2007.

[10] R. Haxaire. Caractérisation et Modélisation des Ecoulements d'Air dans une Serre, Thèse de doctorat, Nice Sophia Antipolis, 1999.

[11] Slimane Lebik, Simulation à L'aide du Code de Calcul CFD des Mécanismes Mis en Jeu dans le RefroidissementEvaporatif Combiné au Renouvellement d'Air dans une Serre, Mémoire de Magistère, Tizi-Ouzou, 2008.

[12] P. K. Kundu-Ira M. Cohen, FluideMécaniques, seconde édition.

[13] B. E. Launder and D. B. Spalding, Lectures in Mathematical Models of turbulence, Academic Press, London, England, 1972.

[14] S. El Mokretar, R. Miri, M. Belhamel, Etude du Bilan d'Energie et de Masse d'un Séchoir de Type Serre, Applications au Séchage des Produits Agro-alimentaires. Rev. Energ. Ren, 7:109-123, 2004.